

# We are IntechOpen, the world's leading publisher of Open Access books Built by scientists, for scientists

6,900

Open access books available

186,000

International authors and editors

200M

Downloads

Our authors are among the

154

Countries delivered to

TOP 1%

most cited scientists

12.2%

Contributors from top 500 universities



WEB OF SCIENCE™

Selection of our books indexed in the Book Citation Index  
in Web of Science™ Core Collection (BKCI)

Interested in publishing with us?  
Contact [book.department@intechopen.com](mailto:book.department@intechopen.com)

Numbers displayed above are based on latest data collected.  
For more information visit [www.intechopen.com](http://www.intechopen.com)



# A Study on Hydrogen Reaction Kinetics of Pt/HfO<sub>2</sub>/SiC Schottky-Diode Hydrogen Sensors

W.M. Tang, C.H. Leung and P.T. Lai

*Department of Electrical and Electronic Engineering,  
The University of Hong Kong, Hong Kong,  
China*

## 1. Introduction

Hydrogen has a wide range of applications and is an essential raw material in many industries such as chemical, food, metallurgical, electronics and others. It can be produced by a variety of methods, including acid and iron methods, steam-reforming production method, coal and electrolysis methods, biological processes, as well as chemical decomposition of hydrogen-containing compounds. Most of the hydrogen produced in the United States is used to synthesize ammonia by the Haber process which can then be used as a soil fertilizer. Hydrogen is also used to produce synthetic methyl alcohol and synthetic petroleum by the Patart method and the Fischer-Tropsch process respectively (Almqvist, 2003). Hydrogen can also be used in the food processing industry to convert vegetable oils into hard and white fats that can be used to make margarine. This process is called hydrogenation, which is the major chemical application of hydrogen. Some oil companies use hydrogenation process to do desulfurization and hydro-cracking. In addition, hydrogen has many industrial applications such as metal smelting, welding, cutting, cooling in power station, electronic fabrication process, fiber optics manufacturing, medical installation and corrosion prevention in nuclear reactors.

The world population rapidly increases nowadays and there is an increasing demand for energy. Fossil fuels are being quickly used up and are not renewable. It has been estimated that the known reserves of petroleum and natural gas will be used up by 2090. Coal deposits are more plentiful but they may last for less than 300 years. It is apparent that mankind is heading toward an energy crisis that can be averted only through conservation coupled with a renewable energy technological revolution. The world must turn to alternative energy sources to meet future energy needs. There are many alternative energy carriers such as solar, wind, tidal, nuclear, etc. Of this wide range of energy carriers, hydrogen is surely one of the most attractive energy carriers. Hydrogen is a clean renewable energy source because it reacts with oxygen producing water only. It causes no air and water pollutions and has a very high fuel value (142 kJ/g). It will be an alternative to fossil fuels in the near future. In most cases, hydrogen is used as a fuel involving the use of fuel cells. Hydrogen can be liquefied at 20.3 K by a multi-stage process, and then liquid hydrogen is easier to store and transport. It can be used for scientific cooling applications and as a rocket fuel for space flights.

Although hydrogen has a lot of useful applications, it has some disadvantages. It can make various metals such as high-strength steels, aluminum, and titanium alloys become brittle and crack. The mechanism starts with hydrogen atoms diffusing through the metal during various manufacturing operations or operational use. These hydrogen atoms will recombine to form hydrogen molecules in the tiny voids of the metal creating a high pressure inside the metal to reduce its ductility and tensile strength. When the pressure is too high, the metal will crack eventually. This process is called hydrogen embrittlement or hydrogen grooving which can pose a serious engineering problem. Hydrogen is also a very dangerous gas. It is highly flammable with a high rate of flame propagation. Its ignition temperature is 500 °C and the explosion range is 4 % to 75 %. The explosion range indicates the amount of hydrogen mixed with air that will cause serious explosions when ignited with a sufficient amount of heat. If hydrogen mixes with air and the concentration of hydrogen is less than 4 %, the mixture is not explosive because there is not enough fuel. The mixture is also not explosive if the mixture contains more than 75 % hydrogen because there will be too much fuel but not enough oxygen for combustion. Only within the lower explosion limit (LEL) and the upper explosion limit (UEL), the H<sub>2</sub>-air mixture burns when ignited, causing significant flame propagation. There is a point within LEL and UEL at which the flame propagation is the greatest (Korver, 2001). As hydrogen poses potential danger, storage and use of hydrogen need special care and attention. In order to avoid the leakage of hydrogen that can cause serious explosion, sensors that can detect hydrogen quickly and accurately are very important and essential in practical applications. Apart from leak detection, monitoring of the hydrogen or hydrocarbon concentration in fuel cell, hydrogen driven vehicle, car exhaust, flue and biomedical and chemical industries is also an important application of hydrogen sensors.

The organization of this chapter is as follows. First, it will briefly review the type of hydrogen sensors and the evolution of Schottky-diode hydrogen sensor. Then, the working principle of Metal-Insulator-Semiconductor (MIS) Schottky-diode hydrogen sensor will be presented. The physical and chemical mechanisms responsible for hydrogen detection will be discussed. Then, it will describe the fabrication procedure of the hydrogen sensors and the measurement methodology. The steady-state and transient behaviour of the Pt/HfO<sub>2</sub>/SiC Schottky-diode hydrogen sensors are then analysed. The sensor response of the device is found to increase with annealing time because longer annealing time can enhance the densification of HfO<sub>2</sub> film and improve the oxide stoichiometry. The hydrogen reaction kinetic and the enthalpy change are then investigated. Finally, the results obtained in this study are summarized.

## 2. Types of hydrogen sensor

There are various types of hydrogen sensors which use different sensing mechanisms to detect hydrogen. Many of them use catalytic metals such as palladium (Pd) or platinum (Pt) as a hydrogen trap because these metals have high hydrogen solubility and can selectively absorb hydrogen gas. The absorption of hydrogen in the catalytic metals depends on temperature and hydrogen concentration. The adsorbed hydrogen gas molecules can dissociate at the Pd or Pt surface to form hydrogen atoms. According to Lundstrom (Lundstrom, 1981), a linear relation can be assumed between the measured response signal

(which can be voltage, pyroelectric signal, frequency shift, optical signal, etc.) and the coverage of hydrogen atoms. Six types of hydrogen sensors are introduced in this section. They are pyroelectric sensors, piezoelectric sensors, fiber-optic sensors, electrochemical sensors, and semiconductor sensors.

### 2.1 Pyroelectric sensor

The first pyroelectric chemical sensor (Pd-LiTaO<sub>3</sub>) was reported in 1981 (Zemel et al., 1981). It makes use of the unique property of pyroelectric material together with a catalyst metal to detect hydrogen. A pyroelectric material can generate an electric potential when it is heated or cooled. A schematic diagram of a pyroelectric hydrogen sensor is shown in Fig. 1. It consists of three main parts: (1) a single-crystal LiTaO<sub>3</sub> wafer which is a pyroelectric material, (2) two NiCr electrodes, one of them is coated with a catalyst material (Pd in this case) and (3) a heater. When hydrogen is introduced into the test cell, it is absorbed by Pd, causing an extra heat gain in the Pd-NiCr electrode and hence a voltage difference between the Pd-NiCr and the reference NiCr electrodes. This type of sensor is not popular because the fabrication procedures are complex and the sensor can be easily influenced by temperature fluctuation due to environmental factors. Besides, the response of the sensor is slow due to the diffusive transport of thermal energy from the Pd electrode to the reference electrode.

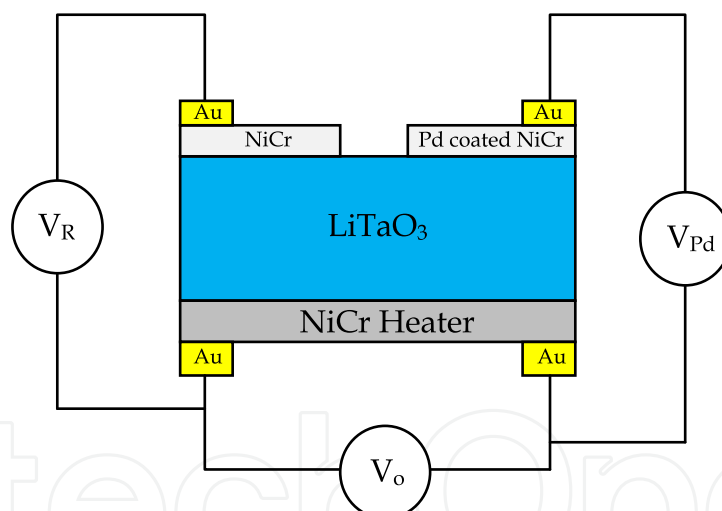


Fig. 1. Schematic diagram of a pyroelectric hydrogen sensor (Christofides et al., 1990).

### 2.2 Piezoelectric sensor

Piezoelectric sensor can be divided into two groups: piezoelectric quartz-crystal microbalance (PQCMB) sensor and surface acoustic wave (SAW) sensor.

#### 2.2.1 Piezoelectric quartz-crystal microbalance (PQCMB) sensor

A coated piezoelectric crystal (e.g. quartz) is very useful for gas detection. The sensing principle was described in 1959 (Christofides, 1990). The setup of the PQCMB sensor is shown in Fig. 2. It consists of an oscillator powered by a regulated power supply and a

frequency meter for measuring the frequency output of the oscillator. The response of the coated PQCMB sensor could be noticed from the change in the resonance frequency of the quartz crystal. The oscillation frequency of the quartz crystal depends on its total mass and the mass of the chemically sensitive layer. When hydrogen molecules are absorbed in the Pd coating layer, the resonance frequency decreases in proportional to the quantity of dissolved molecules. Hence, by observing the change in resonance frequency, the concentration of hydrogen gas can be measured.

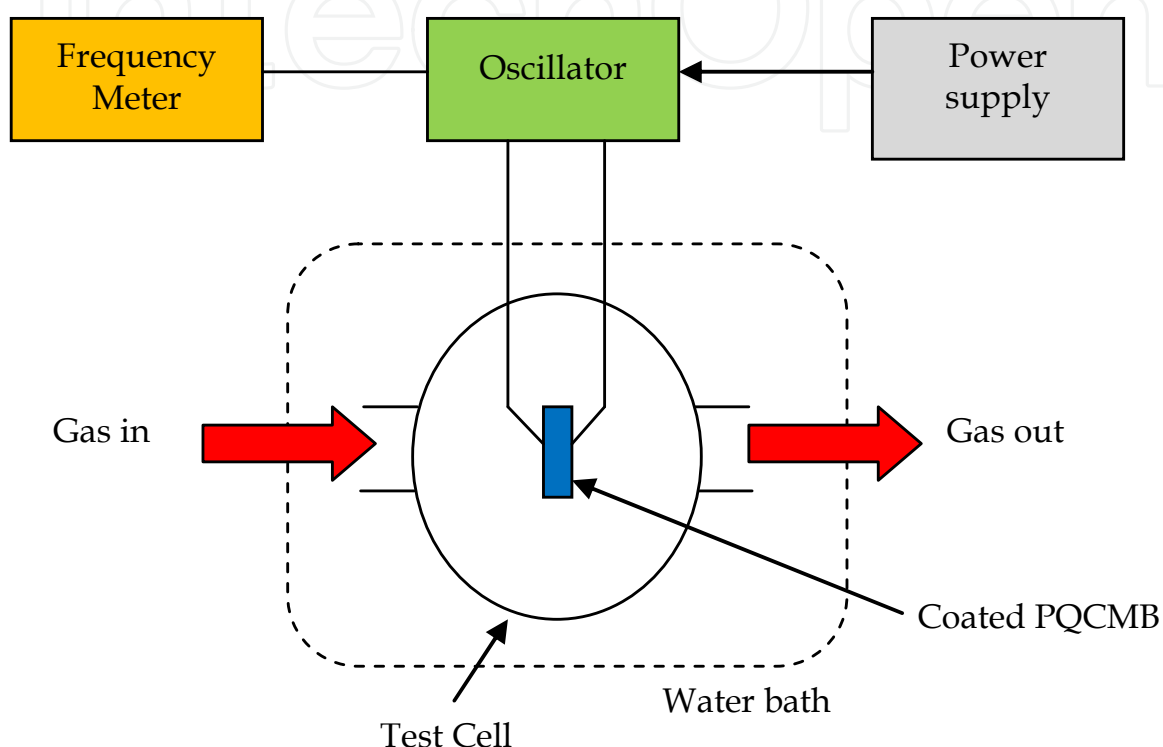


Fig. 2. Setup of the PQCMB sensor (Christofides et al., 1990).

### 2.2.2 Surface acoustic wave (SAW) sensor

The first SAW hydrogen sensor was demonstrated in 1982 (Amico, 1982/83; Amico, 1982), and its sensing mechanism is simple. When hydrogen molecules are absorbed in a Pd or Pt layer, the SAW characteristics such as amplitude, phase, velocity, etc will be changed. A schematic diagram of a SAW hydrogen sensor is shown in Fig.3. The sensor is fabricated on a piezoelectric substrate  $\text{YZ-LiNbO}_3$ . Surface acoustic waves are generated by an input transducer  $T$  and then collected by two output transducers  $T_R$  and  $T_S$ . There are two propagation paths in the device. One path ( $l_S$ ) is coated with a catalyst metal layer (Pd in this case), while the other path ( $l_R$ ) is uncoated as a reference. A double-balance mixer connects the two voltage outputs ( $V_S$  and  $V_R$ ) through inductances  $L_S$  and  $L_R$ . The output from the mixer then goes through a low-pass filter and the differential output voltage  $\Delta S$  ( $V_R - V_S$ ) is filtered out and recorded. When absorption of hydrogen takes place at the Pd surface, a voltage change can be detected. Comparing the two groups of piezoelectric sensor, the SAW sensor has a higher sensitivity than the PQCMB sensor because the former can have a resonance frequency a few hundred times higher.

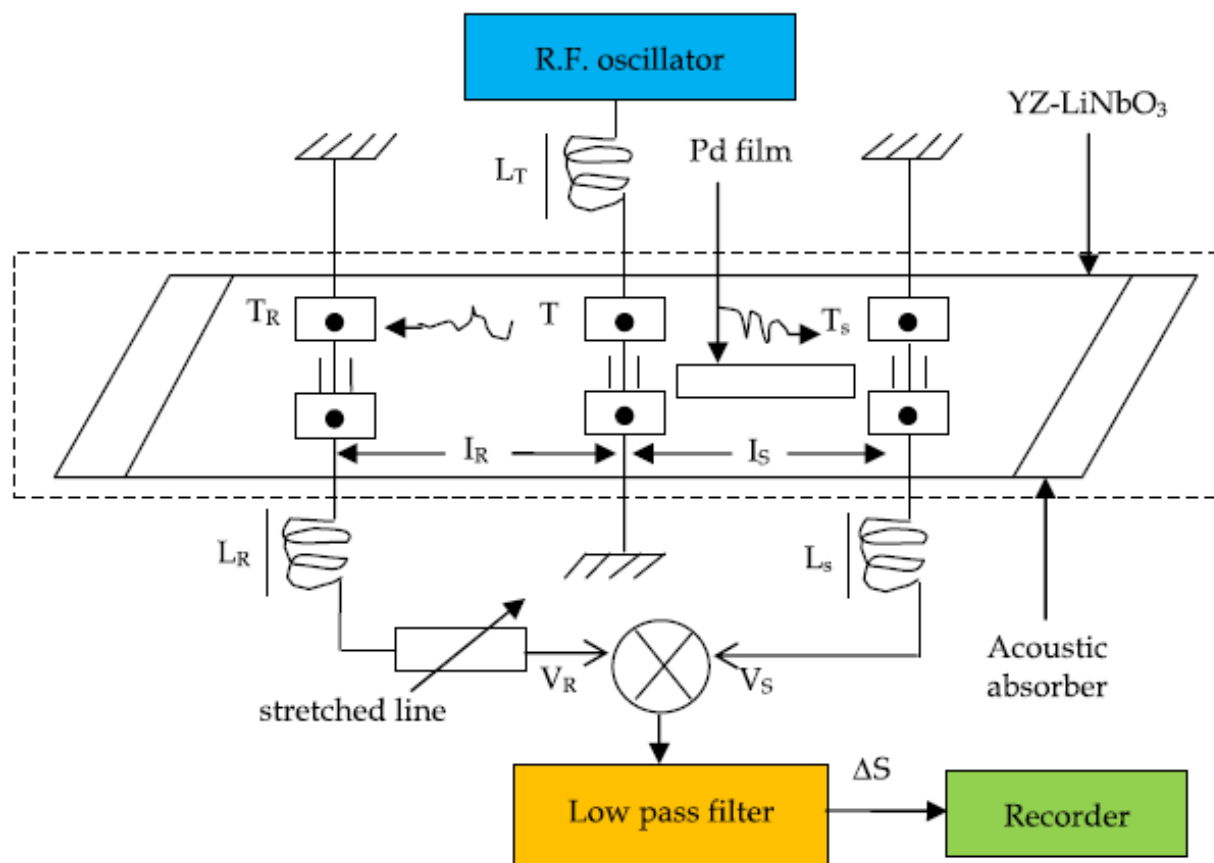


Fig. 3. Schematic diagram of a SAW hydrogen sensor (Amico et al., 1982/83).

### 2.3 Fiber-optic sensor (FOS)

The first FOS to detect hydrogen was developed by Butler in 1984 (Butler, 1984). A schematic diagram of a Pd-coated fiber-optic hydrogen sensor is shown in Fig. 4. Interferometry is applied in this type of sensor. The sensing mechanism of the device is simple and straightforward. When hydrogen molecules are absorbed in the chemically sensitive Pd coating, they will alter the optical properties such as absorbance, reflectance, luminescence, or scattering of the coating. The laser is split into two paths by a beam splitter: one through the Pd-coated fiber and the other through the uncoated fiber. Both ends of the fibers are connected to a quartz plate. When the phase difference between the two interfering beams is  $2n\pi$  ( $n$  is a positive integer), a maximum fringe pattern will appear. A transverse shift in the position of the fringe pattern can be observed when the fibers are exposed to hydrogen gas. The amount of fringe shift is related to the quantity of absorbed species (gas molecules or atoms) in the optical path. The FOS is very useful in environments with considerable electromagnetic activity because the optical nature of the signal does not introduce any electrical interference. However, one drawback for FOS is that the ambient light could interfere with background noise, causing FOS to be preferably used in dark environment for optimal operation and noise minimization.

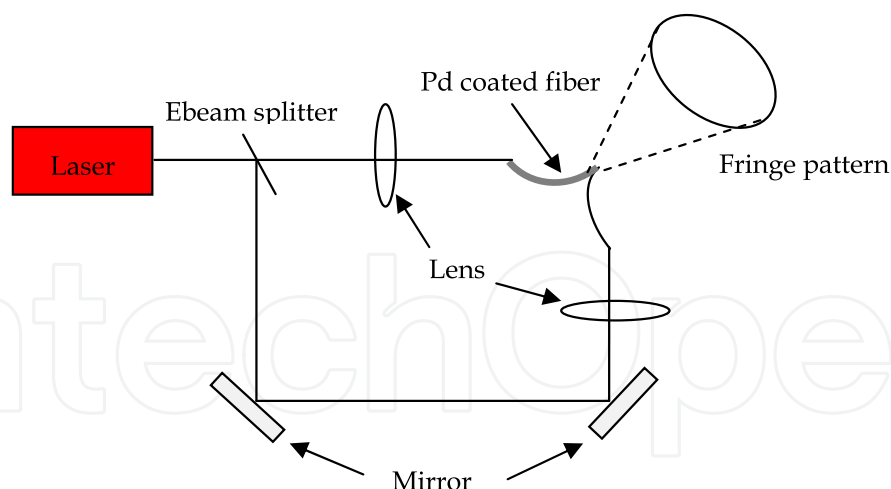


Fig. 4. Schematic diagram of a Pd-coated fiber-optic hydrogen sensor (Butler, 1984).

## 2.4 Electrochemical sensor

The first electrochemical hydrogen sensor was developed in 1978 (Childs et al., 1978). This sensor can be used for the study of hydrogen evolution during the corrosion of copper in pure water. Fig. 5 shows the schematic diagram of the electrochemical hydrogen sensor. The cell consists of a thin reference electrode, a working electrode made of Pt black, and an electrolyte. Hydrogen gas reacts with Pt black at the anode to give out hydrogen atoms and electrons. The potential difference generated in the cell increases linearly with the logarithm of the hydrogen partial pressure. Long response time is a disadvantage of this sensor.

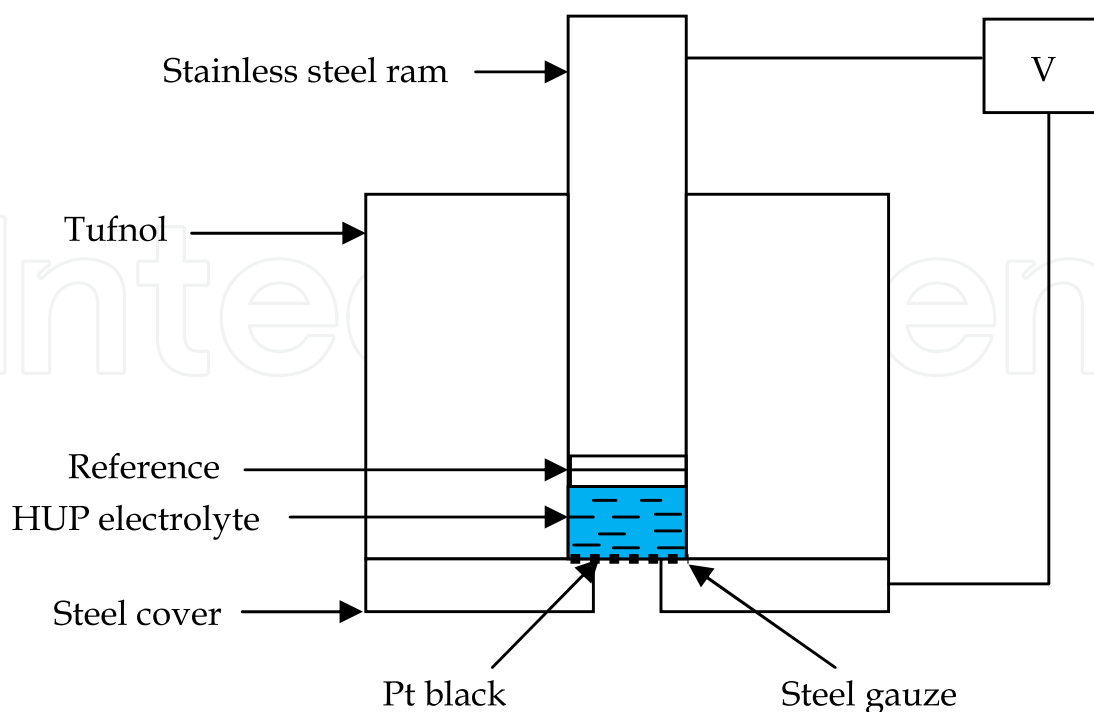


Fig. 5. Schematic diagram of the electrochemical hydrogen sensor (Kumar et al., 1988).

## 2.5 Semiconductor sensor

The detection of hydrogen gas with semiconductor sensors is primarily done with metal-oxide semiconductors. The initial work on this type of sensor can be traced back to the work of Brattain and Bardeen in 1953 (Brattain et al., 1953). The sensing properties of this sensor are based on reactions between oxide semiconductors and gases in the atmosphere. These reactions can change the electrical characteristics of the device. Oxygen in the atmosphere can be absorbed on the semiconductor surface and dissociates to form different species such as O<sub>2</sub>, O<sup>2-</sup> and O<sup>-</sup>, where the electrons are extracted from the semiconductor. This electron extraction increases the resistance of the device (assuming an n-type semiconductor). When the sensor is exposed to a reducing gas such as hydrogen, the hydrogen reacts with the absorbed oxygen species to form water and the electron is re-injected into the semiconductor to reduce the resistance. Several metal-oxide semiconductors have been used as gas-sensing materials such as tin oxide (SnO<sub>2</sub>) (Korotcenko et al., 2001), tungsten trioxide (WO<sub>3</sub>) (Kim et al., 2006), titanium oxide (TiO<sub>2</sub>) (Smith et al., 1993) and zinc oxide (ZnO) (Tomchenko et al., 2003). In order to accelerate the reaction rate and increase the sensitivity, a catalyst Pd or Pt is usually deposited on the surface of the oxide semiconductor. Apart from using catalyst, the sensor performance can be also improved by utilizing nano-structured materials, which have high surface-to-volume ratio for gas absorption. However, expensive equipment, materials and extensive training required to produce nanoscale structures increase the production cost of the sensor and hence limit their practical viability in industrial and commercial applications.

There is another category of semiconductor hydrogen sensor in which the species of interest are adsorbed at the electrode/insulator interface and induce interfacial polarization. The first hydrogen sensor under this category was developed in 1975 (Lundstrom et al., 1975) and was an MOS structure using silicon as substrate, silicon dioxide as gate insulator and palladium as gate electrode. Since then a lot of research on such hydrogen sensors has been done. Different materials and fabrication methods have been used to make the hydrogen sensors (Lundstrom et al., 1989; Spetz et al., 1999; Kim et al., 2000). There are many structures that can be used to make this type of hydrogen sensors, such as metal-oxide-semiconductor field-effect transistor (MOSFET) (Lundstrom et al., 1975), ion-sensitive FET (ISFET) (Bergveld et al., 1972), MOS capacitor (Steele et al., 1976a), Schottky diode (Steele et al., 1976b), etc. When the device is exposed to hydrogen, dissociated hydrogen atoms adsorbed at the electrode-insulator interface are polarized due to the displacement of their negatively-charged electron cloud relative to their positively-charged nucleus by an external applied field. This dipole layer causes a shift of the electrical (*I-V* or *C-V*) characteristics of the device.

## 3. Evolution of Schottky-diode hydrogen sensor

Among the semiconductor hydrogen sensors, Schottky diodes are preferably selected as gas sensors due to its much simpler fabrication procedures and electronic circuitry required for operation. The early Schottky-diode hydrogen sensors often used silicon as substrate because high-quality Si is commercially available and its cost is very low. Silicon is the second most abundant element in the world and is the dominant semiconductor used in the solid-state electronics industry. The properties of silicon have been widely studied and the silicon technology is the most mature and advanced among all semiconductor technologies.

Si-based hydrogen sensors can perform very well at room temperature (Fang et al., 1997) but they can only operate in environment below 250 °C due to the relatively small bandgap of Si (1.12 eV). In order to make these sensors function in harsh environments such as hot-engine and car exhaust, a cooling system is needed. However, this cooling system increases not only the operating and maintenance costs, but also the weight of the whole system, and leaves less space to integrate other electronic components. As a result, the reliability and efficiency of the system become lower. Therefore, development of hydrogen sensors that can directly operate in a high-temperature environment is very useful and important. To achieve this, a new sensor technology based on high-temperature semiconductor materials was then created.

High-temperature semiconductor materials are compound semiconductors such as SiC, CdS, GaP, AlN, GaN, etc with larger bandgap and thus lower intrinsic carrier concentration, which enables them to operate at much higher temperatures than silicon. Devices made of wide-bandgap materials can operate potentially up to 1000 °C. Thus, they are very suitable for making hydrogen sensors for aerospace and automobile applications, process-gas monitoring and leak detection. Uncooled operation of these sensors enables significant reductions in aircraft weight, operating and maintenance costs, overall system size, pollution, and also increases in operational safety, efficiency and reliability. Among the wide-bandgap materials, silicon carbide is by far the most developed for use in high-temperature, high-power, and high-radiation conditions. It is because sublimation growth of SiC wafer has been developed and high-quality 4H- and 6H-SiC wafers have been commercially available by Cree Research since 1989. These greatly facilitate the development of SiC semiconductor electronics. Besides, SiC can make good ohmic and Schottky contacts with a wide range of metals. It can also allow high-quality insulator (SiO<sub>2</sub>) grown on top of it when it is put in an oxygen environment at high temperature. In addition, patterned etching of SiC has been developed for device fabrication. The electrical, optical, and physical properties of SiC have been extensively studied. With a wider bandgap, SiC not only can make gas sensor for emissions monitoring applications (Hunter et al., 1998; Spetz et al., 1997) but also has the capability to make blue pn-junction light-emitting diodes (LEDs) (Kong et al., 1997). High breakdown field, high saturation velocity together with high thermal conductivity allow SiC-based devices to function properly in high-power-density and high-frequency environments. Moreover, SiC has excellent mechanical properties because it is extremely hard, refractory and rustless. The first SiC Schottky-diode hydrogen sensor was developed by Hunter at NASA Lewis Research Center in 1992 (Hunter et al., 1992). It was a simple Schottky-diode structure, which had a catalytic metal Pd directly deposited on SiC. This sensor structure could sensitively detect hydrogen but was not thermally stable (Hunter et al., 1995; Chen et al., 1996). After this structure was heated for a long time, there were interfacial reactions between Pd and SiC, forming Pd silicides (Hunter et al., 1995) and causing a shift in sensor properties (Hunter et al., 1997). To provide long-term high-temperature stability, different materials, fabrication techniques and sensor structures were developed. NASA Lewis Research Center and Case Western Reserve University used alloys such as palladium chrome as the catalytic metal (Hunter et al., 1998) while some researchers employed more thermally stable metallization such as tungsten. Diamond, amorphous and polycrystalline barium strontium titanate (BST) have been used as a substrate to reduce the interfacial reaction (Kang et al., 1995; Chen et al., 2000; Dietz et al., 1997). A Metal-Insulator-Semiconductor (MIS) structure involving the use of a gate

insulator was developed to suppress the interfacial diffusion between the electrode and the substrate, and hence can make the device more stable for gas sensing. Several gate insulators such as SnO<sub>2</sub> (Hunter et al., 2000) and SiO<sub>2</sub> (Chen et al., 1997; Zangoie et al., 2000; Tobias et al., 1997) have been used. These gate insulators provide some improvements on the sensor performance but they are still not very stable after long-duration high-temperature operation (Hunter et al., 2000). Since the sensitivity and stability of the sensor largely depend on the gate insulator, development of a high-quality gate insulator for MISiC Schottky sensors has become an essential issue. SiO<sub>2</sub> growth in NO gas was then developed to improve the oxide reliability and reduce the interface states and oxide charges (Xu et al., 2003). A technique of growing the oxide layer in O<sub>2</sub> and trichloroethylene (TCE) was also employed to fabricate a hydrogen sensor (Tang et al., 2005). This sensor demonstrated excellent H<sub>2</sub>-sensitive properties due to the passivation effect of Cl<sub>2</sub> or HCl at the SiO<sub>2</sub>/SiC interface. Researchers are continually seeking new materials and methods to produce more sensitive, stable and reliable sensors, which can function at higher temperature for a longer period of time.

#### 4. Working principle of MIS Schottky-diode hydrogen sensor

A schematic representation of a MISiC Schottky-diode hydrogen sensor is shown in Fig. 6. It consists of three main parts: (1) the substrate, (2) the gate insulator and (3) the front electrode.

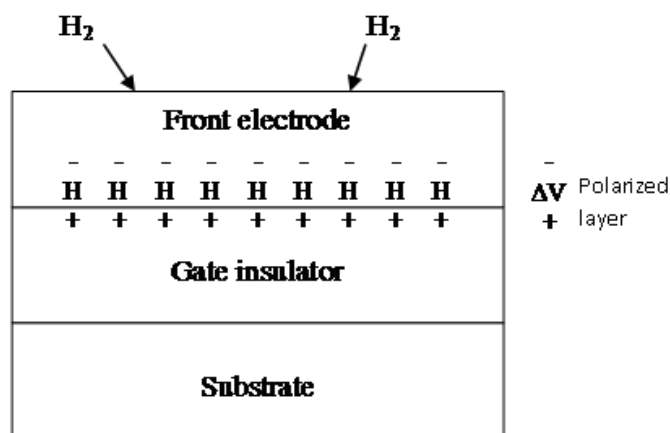


Fig. 6. Schematic representation of a MISiC Schottky-diode hydrogen sensor.

When hydrogen-containing molecules come to the catalytic gate metal, they dissociate on the surface of the metal and form hydrogen atoms. These hydrogen atoms then diffuse through the metal in the order of nano- to microseconds to the insulator surface, and form a polarized layer (see Fig. 6) at the electrode-insulator interface (Ekedahl et al., 1998). This polarized layer reduces the potential barrier at the electrode-insulator interface, and hence leads to a shift in the *I-V* curve of the Schottky diode. The amount of voltage shift at a fixed current is assumed to be proportional to the atomic hydrogen concentration at the interface or the hydrogen coverage  $\theta_i$ . The maximum voltage change  $\Delta V_{max}$  occurs when each hydrogen absorption site at the interface is occupied by one hydrogen atom, i.e. the

hydrogen coverage is one. The hydrogen coverage at a certain hydrogen concentration depends on two processes. One process is hydrogen dissociation, by which hydrogen atoms diffuse through the metal and are blocked at the interface. The other process is the way hydrogen flows out back to the ambient. Hydrogen atoms at the metal surface can recombine together to form hydrogen molecules or react with oxygen species to form water molecules. Hence, at steady state, the actual coverage of hydrogen at the interface is a result of a balance between these two processes. Fig. 7 shows the schematic energy-band diagram for a MISiC Schottky-diode hydrogen sensor. Electrons in the conduction band of the substrate (SiC) have to overcome an energy barrier  $\phi_b$  to reach the gate (Pt). The polarized hydrogen layer can increase the electron concentration of the metal and hence its Fermi level near the insulator layer. As a result, the lower energy barrier at the metal-insulator interface increases the forward current of the device. The above sensing mechanism is a reversible process because the hydrogen atoms adsorbed at the electrode/insulator interface can diffuse out of the interface to the surface of the electrode and finally recombine together to form hydrogen gas. Thus, when the introduction of hydrogen to the sensor is stopped, the sensor will return to its initial condition after some time. The reactivity and solubility of hydrogen are different for different catalytic metals (Lechuga et al., 1992). MISiC sensors with porous catalytic metal have higher sensitivity to detect gases because they have larger active surface areas available for hydrogen adsorption (Lechuga et al., 1992; Spetz et al., 2000).

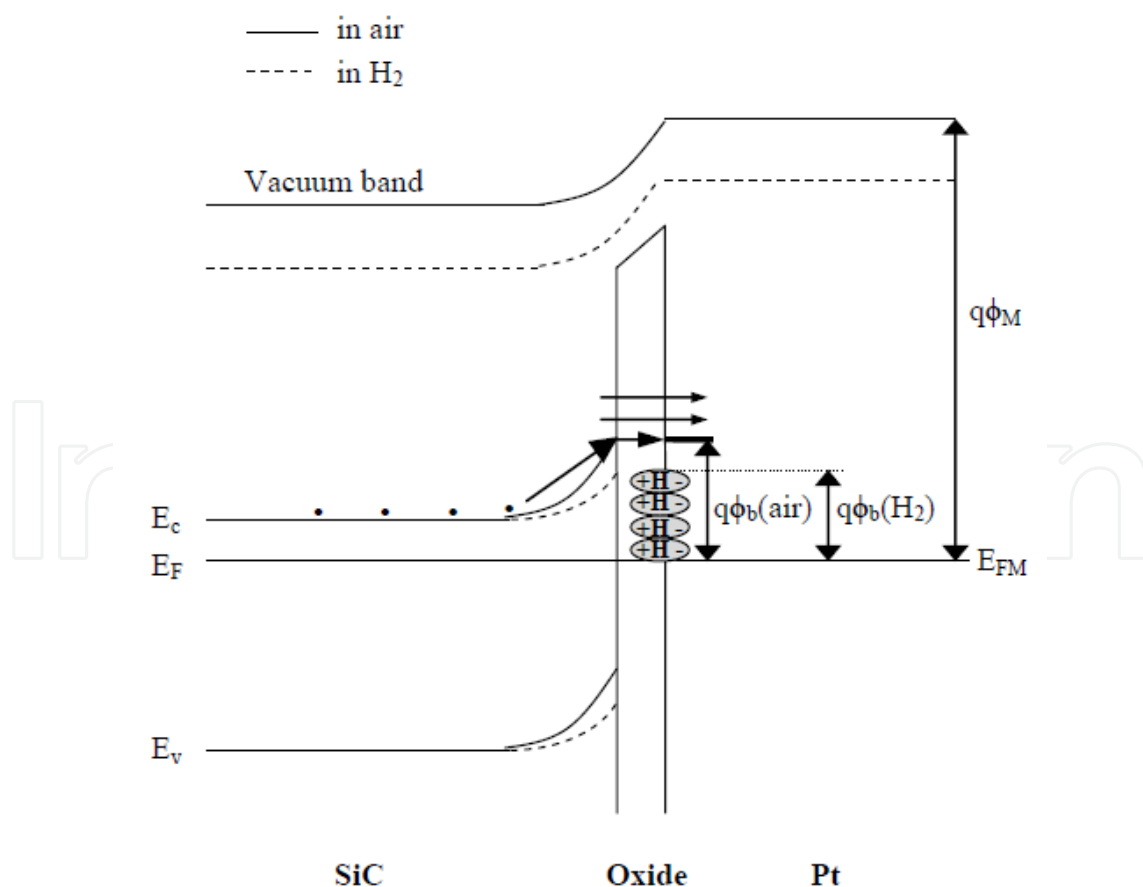


Fig. 7. Schematic energy-band diagram for a MISiC Schottky-diode hydrogen sensor.

## 5. Experimental details

### 5.1 Fabrication procedures of the hydrogen sensors

N-type (0001) Si-face 4H-SiC wafer, manufactured by CREE Research, was used in this study. The SiC wafer had a 5- $\mu\text{m}$  epitaxial layer grown on heavily doped substrate. The doping level of the epitaxial layer was  $5\text{-}6 \times 10^{15} \text{ cm}^{-3}$ . The wafer was cleaned using the conventional Radio Corporation of America method followed by a 60 sec dipping in 5% hydrofluoric acid to remove the native oxide. The wafer was then loaded into a Denton vacuum LLC Discovery 635 sputterer, which was then pumped down to  $2.67 \times 10^{-4} \text{ Pa}$ . The most promising high-k dielectric for Si technology, hafnium oxide HfO<sub>2</sub>, was chosen as the gate insulator of the MISiC sensor as such sensor showed much higher sensitivity than its SiO<sub>2</sub> counterpart (Tang et al., 2008). HfO<sub>2</sub> was deposited at room temperature by DC sputtering of hafnium metal (99.99 % purity) with a sputtering power of 17.52 W in a mixed Ar/O<sub>2</sub> ambient (Ar to O<sub>2</sub> ratio 4:1) for 20.9 min. An electrode consisting of 100-nm Pt with a diameter of 0.5 mm was then deposited on the wafer by DC-magnetron sputtering through a stainless steel shadow mask. The sample then underwent an annealing by loading it into a furnace at 650 °C in N<sub>2</sub> (1000 ml/min) for 5 min (denoted as H05 sample). In order to investigate the effects of annealing time on the sensor performance, two more hydrogen sensors annealed under the same annealing gas but with different annealing durations were fabricated. The sample annealed at 650 °C for 10 min was denoted as H10 sample while the one annealed for a longer time (60 min) was denoted as H60 sample. The oxide at the back of the wafers was removed using 20 % HF solution. The back of the SiC wafer was then pasted using silver epoxy on a gold-coated header with one pin as the back contact. The header was then put into an oven at 200 °C for half an hour to harden the silver epoxy. Lastly, a gold wire was connected between the Pt electrode and one of the pins of the header using a hybrid wedge bonder. The hydrogen sensor fabricated in this study is shown in Fig. 8.



Fig. 8. Photograph of three hydrogen sensors bonded on a header.

### 5.2 Measurement methodology

The hydrogen-sensing properties of the samples were compared with each other by taking measurements under various temperatures and hydrogen concentrations using a computer-controlled measurement system (See Fig. 9). This measurement system mainly consisted of

two parts: the gas-mixing supply system and the parameter-testing system. The test sample was placed in a stainless steel reaction chamber enclosed by the thermostat and gases were injected into the reaction chamber through the digital gas flow controllers (DFCs). The thermostat, the HP 4145B semiconductor parameter analyzer and the DFCs were all connected to a computer and were controlled by computer programs. The computer programs could provide different measurement conditions and the measurement results were automatically saved in the computer.

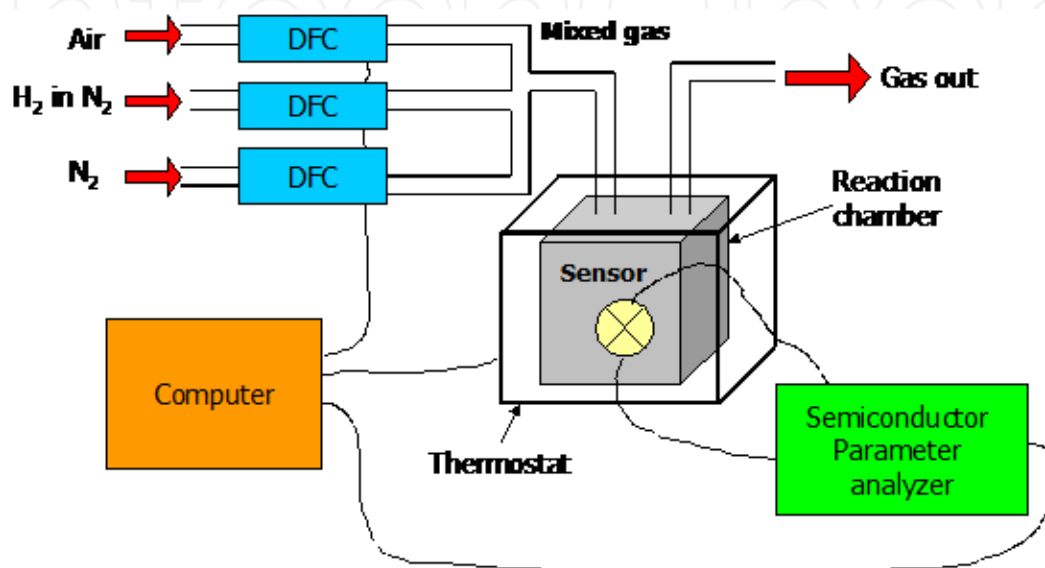


Fig. 9. Computer-controlled measurement system.

## 6. Results and discussion

Fig. 10 shows the  $I$ - $V$  curves of the H60 sample measured in air and in different hydrogen concentrations (238 ppm, 429 ppm and 619 ppm) at 50 °C and 150 °C. The  $I$ - $V$  curve shifts to the left as temperature increases. The hydrogenation effect becomes more obvious at 150 °C. The  $I$ - $V$  curves shift to the left as hydrogen concentration increases. The shift toward a lower voltage is due to the formation of a polarized layer at the electrode-insulator interface. The  $I$ - $V$  curves of the H05, H10 and H60 samples measured in air and in 48 ppm  $H_2$  in  $N_2$  at 450 °C are compared in the inset of Fig. 10. Among the three studied devices, the H60 sample has the largest current variation ( $\Delta I$ ) measured at a fixed bias voltage.

Fig. 11 depicts the sensor response of the H60 sample upon exposure to different  $H_2$  concentrations in  $N_2$  at several operating temperatures. The sensor response is defined as  $(I_{H_2} - I_{air})/I_{air}$ , where  $I_{H_2}$  and  $I_{air}$  are currents measured under hydrogen environment and air respectively. The response signal of the H60 sample increases with hydrogen concentration and temperature. When temperature increases, the hydrogen under higher pressure will bombard the surface of the electrode more frequently. Hence, more hydrogen molecules can adsorb at the surface of the electrode and decompose into hydrogen atoms. More hydrogen atoms diffuse through the metal layer to the metal/insulator interface to form a polarized layer. This stronger polarized layer gives a larger barrier-height reduction, thus increasing the sensor response. Increasing  $H_2$  concentration can also cause more hydrogen atoms

adsorb at the metal-insulator interface to produce a stronger dipole layer, resulting in more barrier-height lowering, and thus higher sensor response. The inset of Fig. 11 compares the sensor response of the H05, H10 and H60 samples upon exposure to different H<sub>2</sub> concentrations in N<sub>2</sub>. It is found that extending the annealing duration can increase the sensor response of the hydrogen sensors because it can enhance the quality of the HfO<sub>2</sub>/SiC interface and improve the dielectric properties of the HfO<sub>2</sub> film to produce larger barrier-height modulation and to give smaller  $I_{air}$ .

Fig. 12 shows the adsorption transient behaviour of the H60 sample upon exposure to 800-ppm H<sub>2</sub> in N<sub>2</sub> at 50 °C, 150 °C and 450 °C for a bias voltage of 2.5 V. The current shift increases with hydrogen concentration and temperature because more hydrogen-containing molecules adsorbed at the electrode-insulator interface can form a stronger polarized layer to give a larger current shift. The response time which is defined as  $e^{-1}$  times the final steady-state value can be obtained from the transient-response curve. The response time of the H60 sample at 50 °C, 150 °C and 450 °C is 25, 13 and 9 sec respectively. The response time of the hydrogen sensor decreases with the increasing operating temperature because high temperature enables faster hydrogen decomposition and diffusion, and hence faster response. The current–time ( $I-t$ ) characteristics of the H05, H10 and H60 samples at 450 °C are shown in the inset of Fig. 12. These curves can be used to obtain the current shift ( $I_{H_2} - I_{air}$ ) and thus sensitivity of each sample. The measured data shows that the H60 sample has the highest sensitivity while the H10 sample has the lowest.

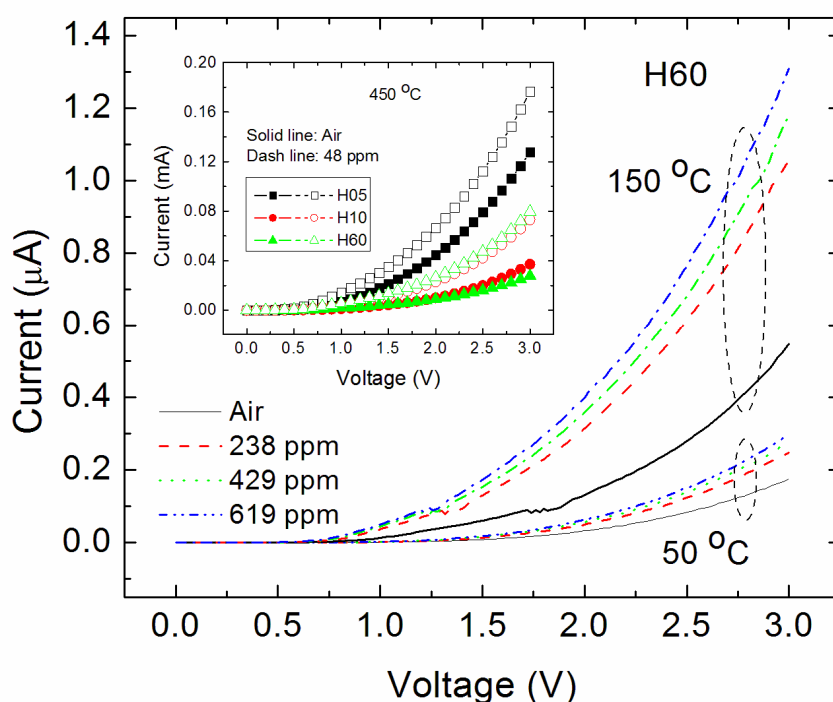


Fig. 10.  $I-V$  curves of the H60 sample measured in air and in different hydrogen concentrations at 50 °C and 150 °C. The inset shows the  $I-V$  curves of the H05, H10 and H60 sample at 450 °C.

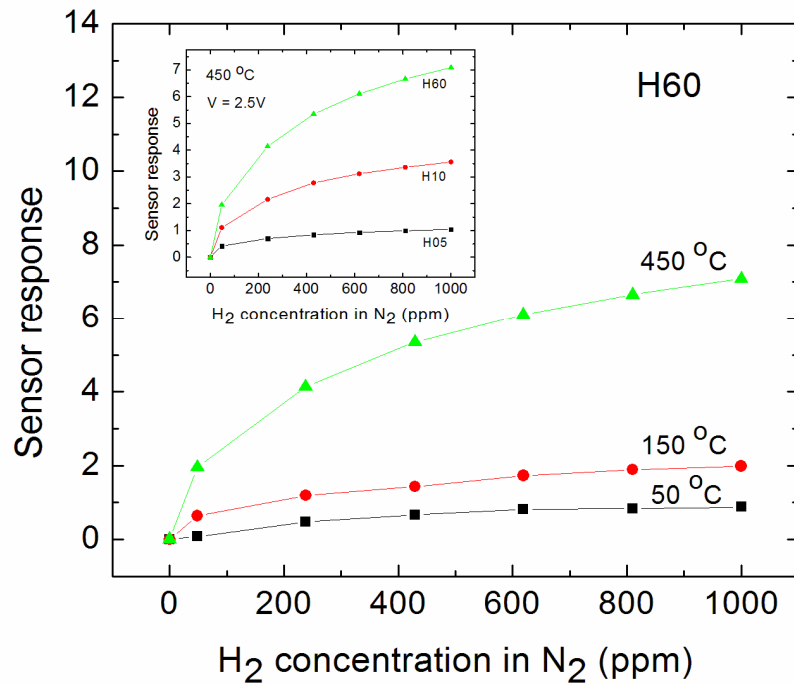


Fig. 11. Sensor response of the H60 sample upon exposure to different H<sub>2</sub> concentrations in N<sub>2</sub> at several operating temperatures (bias voltage  $V = 2.5$  V). The inset compares the sensor response of the H05, H10 and H60 samples at 450 °C.

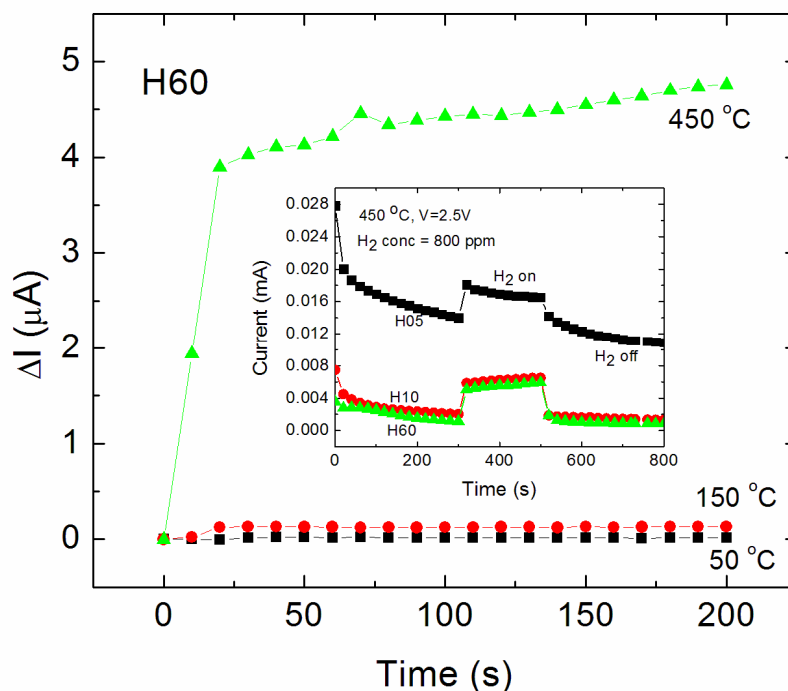


Fig. 12. Adsorption transient behaviour of the H60 sample upon exposure to 800-ppm H<sub>2</sub> in N<sub>2</sub> at 50 °C, 150 °C and 450 °C. The  $I$ - $t$  characteristics of the H05, H10 and H60 samples at 450 °C are shown in the inset.

According to the hydrogen reaction kinetics (a mathematical model that describes the characteristics and mechanism of chemical reactions happened to hydrogen moving from the electrode surface to the electrode/insulator interface), the hydrogen coverage  $\theta$  at the interface under steady-state condition can be written as (Johansson et al., 1998)

$$\theta/(1 - \theta) = k_o (P_{H_2})^{1/2} \quad (1)$$

where  $k_o$  is a temperature-dependent constant which depends on the difference of adsorption between the surface and interface and  $P_{H_2}$  is the hydrogen partial pressure. The change in voltage across the hydrogen dipole layer  $\Delta V$  is proportional to the hydrogen coverage (i.e.  $\Delta V \propto \theta$ ) and the proportionality constant is  $\Delta V_{max}$  (maximum voltage change at a fixed temperature). By substituting  $\theta = \Delta V/\Delta V_{max}$  into equation (1),

$$1/\Delta V - 1/\Delta V_{max} = [k_o \Delta V_{max} (P_{H_2})^{1/2}]^{-1} \quad (2)$$

By using the equation  $\ln I = \ln I_o + qV/(nkT)$ , where  $k$  is the Boltzmann constant,  $T$  the temperature in  $K$ ,  $n$  the ideality factor,  $I_o$  the saturation current, and  $q$  the elementary charge, equation (2) can be written as

$$1/\ln(I_{og}/I_o) = [\ln(I_{ogmax}/I_o)]^{-1} \{1 + [k_o (P_{H_2})^{1/2}]^{-1}\} \quad (3)$$

where  $I_{og}$  and  $I_{ogmax}$  are respectively the saturation current and maximum saturation current of the sensor in hydrogen environment. Under air ambient, the partial pressure of oxygen is 21.4 kPa. As can be seen in Fig. 13, the plot of  $1/\ln(I_{og}/I_o)$  versus  $(1/P_{H_2})^{1/2}$  is a straight line, thus confirming the hydrogen reaction kinetics in the H05, H10 and H60 samples. From the slope and y-intercept of the plot,  $k_o$  is calculated and shown in the inset table of Fig. 13. It is found that the H60 sample has the largest  $k_o$ . Fig. 14 shows the plot of  $1/\ln(I_{og}/I_o)$  vs  $(1/P_{H_2})^{1/2}$  for the H60 sample at different temperatures (50 °C, 150 °C, and 450 °C). The  $k_o$  value increases with increasing operating temperature. According to the van't Hoff equation (Silbey et al., 2001)

$$\ln k_o = -\Delta H^o/RT + \Delta S_o/R \quad (4)$$

where  $\Delta H^o$  is the enthalpy change;  $\Delta S_o$  is the entropy change; and  $R$  is the gas constant (8.314472 JK<sup>-1</sup>mol<sup>-1</sup>). Fig. 15 illustrates a plot of  $\ln k_o$  versus  $1/T$  for the H60 sample. From the slope of the plot, the enthalpy change is determined as 1.18 kJ/mol. Since the hydrogen adsorption process is endothermic, it is favorable for high-temperature detection.

## 7. Conclusion

MISiC Schottky-diode hydrogen sensors with HfO<sub>2</sub> gate insulator annealed in N<sub>2</sub> at 450 °C for different durations have been fabricated and studied. Steady-state and transient-response measurements at different temperatures and hydrogen concentrations are carried out using a computer-controlled measurement system. Measured data are then used to investigate the sensitivity and response speed of the sensors. By analyzing the data, the hydrogen-reaction kinetic of the devices is deduced. Experimental results show that the sensitivity increases with the N<sub>2</sub>-annealing time. Longer annealing duration can enhance the

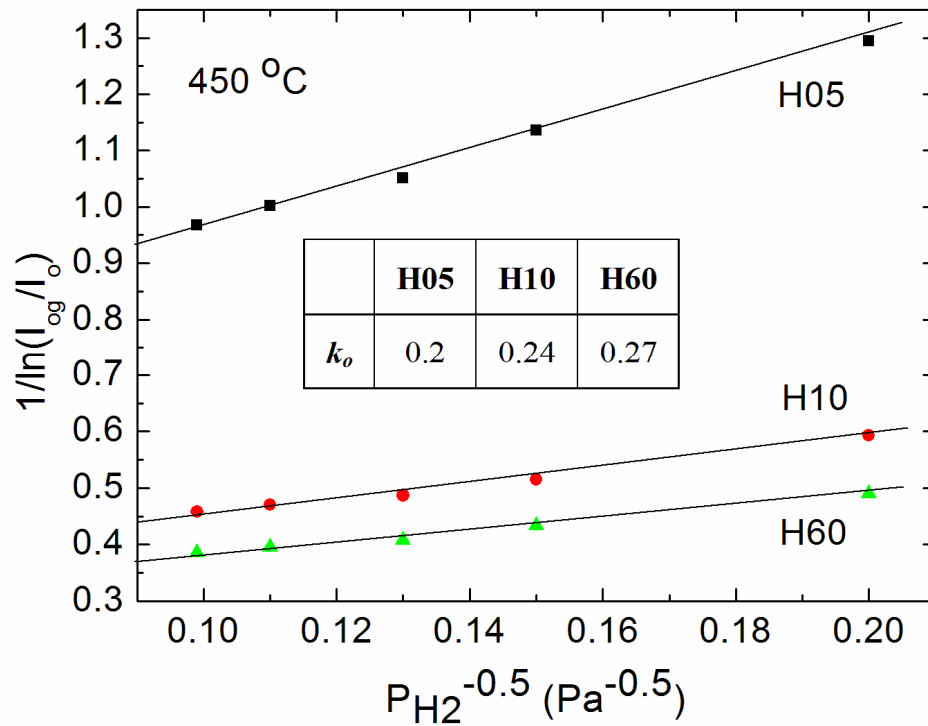


Fig. 13. Steady-state reaction kinetic analysis for hydrogen absorption of H05, H10 and H60 samples at 450 °C.

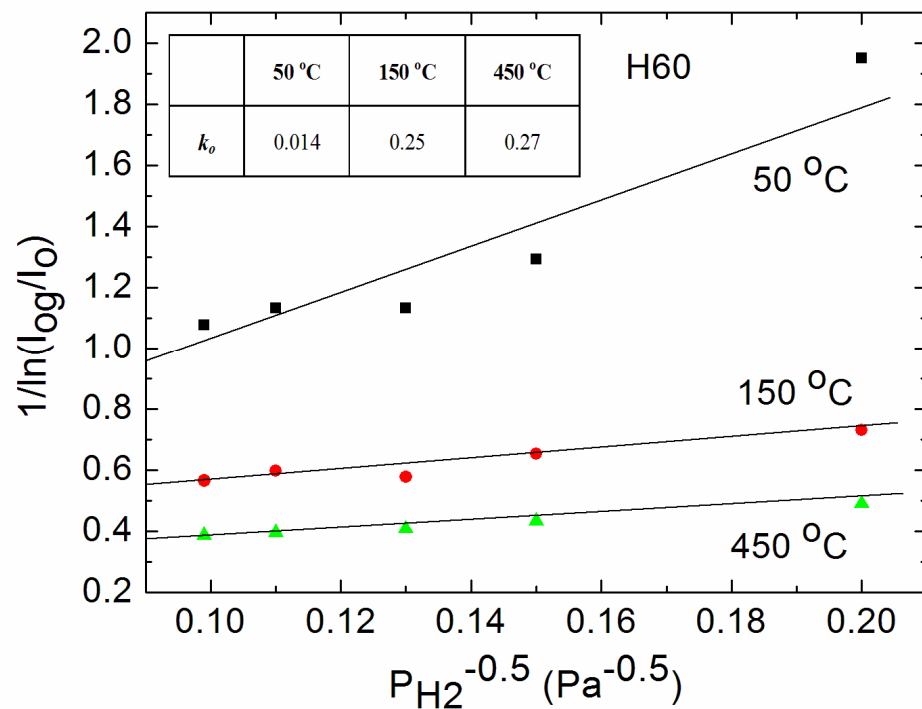


Fig. 14. Plot of  $1/\ln(I_{og}/I_o)$  vs  $(1/P_{H_2})^{1/2}$  for the H60 sample at different temperatures (50 °C, 150 °C, and 450 °C).

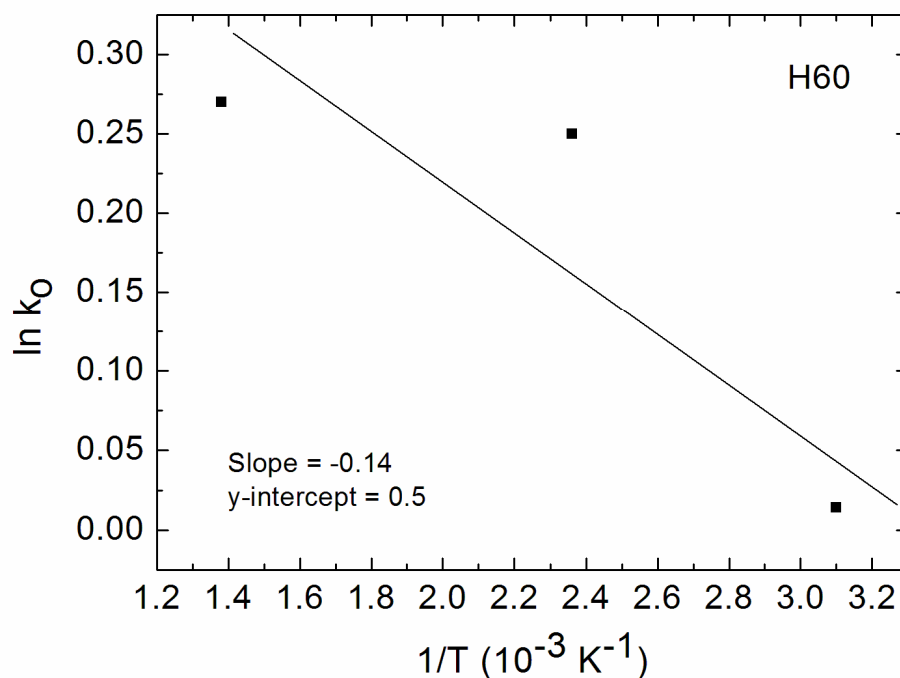


Fig. 15. Plot of  $\ln k_0$  versus  $1/T$  for the H60 sample.

densification of the HfO<sub>2</sub> film; improve the oxide stoichiometry; and facilitate the growth of the interfacial layer, thus causing a remarkable reduction of  $I_{air}$  and thus higher sensitivity. It is also found that the response time of the hydrogen sensor decreases by 64 % as the operating temperature increases from 50 °C to 450 °C. In addition, according to the hydrogen kinetic analysis, the temperature-dependent constant of the Pt/HfO<sub>2</sub>/SiC Schottky diode hydrogen sensor decreases as the operating temperature increases. This indicates that the atomic hydrogen concentration at the interface or the hydrogen coverage  $\theta$  at the Pt/HfO<sub>2</sub> interface increases at higher temperature. Moreover, the positive enthalpy change obtained from the kinetic analysis implies that the hydrogen adsorption process is endothermic.

## 8. Acknowledgment

We would like to acknowledge the University Development Fund (Nanotechnology Research Institute, 00600009) of the University of Hong Kong and RGC of HKSAR, China (Project No. HKU 713310E).

## 9. References

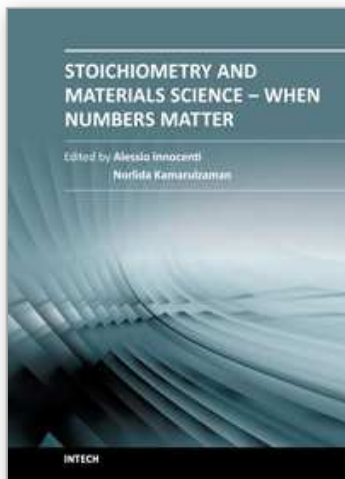
- Almqvist, E. (2003). *History of Industrial Gases*, Kluwer academic/plenum publishers
- Bergveld, P. (1972). Development, operation, and application of the ion-sensitive field-effect transistor as a tool for electrophysiology. *IEEE Trans. Biomed. Eng.*, Vol. BME-19, pp. 342-351

- Brattain, W. H. & Bardeen, J. (1953). Surface properties of germanium, *Syst. Tech. J.*, Vol. 32, No. 1, pp. 1-41
- Butler, M. A. (1984). Optical fiber hydrogen sensor. *Appl. Phys. Lett.*, Vol. 45, pp.1007-1009
- Korver, W.O.E. (2001). *Electrical Safety in Flammable Gas/Vapor Laden Atmospheres*, William Andrew
- Chen, L.-Y., Hunter, G.W., Neudeck, P.G., Bansal, G., Petit, J.B., Knight, D., Liu, C.-C. & Wu, Q.H. (1996). Electronic and interfacial properties of Pd/6H-SiC Schottky diode gas sensors, *Proceedings of the Third International High Temperature Electronics Conference*, Albuquerque, NM
- Chen, L.-Y., Hunter, G.W., Neudeck, P.G. (1997). Comparison of interfacial and electronic properties of annealed Pd/SiC and Pd/SiO<sub>2</sub>/SiC Schottky diodes. *J. Vac.Sci.Technol.A*, Vol.15, pp. 1228-1234
- Chen, X. F., Zhu, W. G. & Tan, O. K. (2000). Microstructure, dielectric properties and hydrogen gas sensitivity of sputtered amorphous Ba<sub>0.67</sub>Sr<sub>0.33</sub>TiO<sub>3</sub> thin film. *Materials Science and Engineering B*, Vol. B77 pp. 177-184
- Childs, P. E., Howe, A. T. & Shilton, M. G. (1978). Battery and other applications of a new proton conductor: hydrogen uranyl phosphate tetrahydrate, H<sub>2</sub>UO<sub>2</sub>PO<sub>4</sub>·4H<sub>2</sub>O. *J. Power Sources*, Vol. 3, pp. 105-114
- Christofides, C. & Mandelis, A. (1990). Solid-state sensors for trace hydrogen gas detection. *J. Appl. Phys.*, Vol. 68, No. 6, pp. R1-30
- D'Amico, A., Palma, A. & Verona, E. (1982/83). Surface Acoustic-Wave Hydrogen Sensors. *Sensors and Actuators*, Vol. 3, pp. 31-32
- D'Amico, A., Palma, A. & Verona, E. (1982). Palladium-surface acoustic wave interaction for hydrogen detection. *Appl. Phys. Lett.*, Vol. 41, pp. 300-301
- Dietz, G. W., Schumacher, M., Waser, R., Streiffer, S. K., Basceri, C. & Kingon, A. I. (1997). Leakage currents in Ba<sub>0.67</sub>Sr<sub>0.33</sub>TiO<sub>3</sub> thin films for ultrahigh-density dynamic random access memories, *J. Appl. Phys.* vol. 82 pp. 2356
- Edmond, J., Suvorov, A., Waltz, D. & Carter, C. (1997). 6H-Silicon Carbide Light Emitting Diodes and UV Photodiodes. *Physica Status Solidi (a)*, Vol. 162, p. 481
- Ekedahl, L.-G., Eriksson, M., Lundstrom, I. (1998). Hydrogen sensing mechanisms of metal-insulator interfaces. *Acc. Chem. Res.* Vol. 31, No. 5, pp. 249-256
- Fang, Y. K., Hwang, S. B., Lin, C.Y. & Lee, C.C. (1997). Trench Pd/Si metal-oxide-semiconductor Schottky barrier diode for a high sensitivity hydrogen gas sensor. *J. Appl. Phys.*, Vol. 82, pp. 3143-3146
- Hunter, G. W., Neudeck, P. G., Jefferson, G. D. (1992). The development of hydrogen sensors technology at NASA Lewis Research Centre, *4<sup>th</sup> Ann. Space System Health Management Technology Conference*
- Hunter, G.W., Neudeck, P.G., Chen, L.-Y., Knight, D., Liu, C.-C. & Wu, Q.H. (1995). Silicon Carbide-Based Hydrogen and Hydrocarbon Gas Detection, *1<sup>st</sup> Joint Propulsion Conference and Exhibit*, San Diego, CA
- Hunter, G.W., Neudeck, P.G., Chen, L.-Y. (1997). SiC-based Schottky diode gas sensor. *7<sup>th</sup> Int. conf. Silicon Carbide, III-Nitrides and Related Materials*, Stockholm, Sweden, *Trans.Tech.*, Vol.2, pp. 1093-1096
- Hunter, G.W., Neudeck, P.G., Chen, L.Y., Knight, D., Liu, C. C. & Wu, Q.H. (1998). Microfabricated chemical sensors for safety and emission control applications. *Proc. 17<sup>th</sup> Digital Avionics Systems Conf.*, Vol. 1, pp. D11/1-D11/8

- Hunter, G. W., Neudeck, P. G., Chen, L. Y., Knight, D., Liu, C. C. & Wu, Q. H. (1998). SiC-Based Schottky Diode Gas Sensors, *Silicon Carbide, III-Nitrides, and Related Materials. Materials Science Forum*, 264-268
- Hunter, G.W., Neudeck, P.G., Gray, M. (2000). SiC-based gas sensor development. *Materials Science Forum*, Vol. 338-342, pp. 1439-1442
- Johansson, M., Lundstrom, I., Ekedahl, L.-G. (1998). Bridging the pressure gap for palladium metal-insulator-semiconductor hydrogen sensors in oxygen containing environments. *J. Appl. Phys.*, Vol. 84, No. 1, pp. 44-51
- Kang, W. P., Gurbuz, Y., Davidson, J. L. & Kerns, D. V. (1995). A polycrystalline diamond thin-film-based hydrogen sensor. *Sensors and Actuators B*, Vol 24-25, pp. 421-425
- Kim, C.K., Lee, J.H., Chow, N.I. & Kim, D.J. (2000). A study on a platinum-silicon carbide Schottky diodes as a hydrogen gas sensor. *Sensors and Actuators B*, Vol. 66, pp. 116-118
- Kim, H. S., Moon, W. T., Jun, Y. K. & Hong, S. H. (2006). High H<sub>2</sub> sensing performance in hydrogen trititanate-derived TiO<sub>2</sub>. *Sensors and Actuators B*, 120, pp. 63-68
- Korotcenko, G., Brinzari, V., Schwank, J., DiBattista, M. & Vasiliev, A. (2001) Peculiarities of SnO<sub>2</sub> thin film deposition by spray pyrolysis for gas sensor application. *Sensors and Actuators B*, Vol. 77, pp. 244-252
- Kumar. R.V. & Fray, D.J. (1988). Development of solid-state hydrogen sensors. *Sensors and Actuators*, Vol. 15, No. 2, pp. 185-191
- Lechuga, L. M., Calle, A., Golmayo, D., Briones, F. (1992). Different catalytic metals (Pt, Pt, and Ir) for GaAs Schottky barrier sensors. *Sensor and Actuators B, Chem.*, Vol. 7, pp. 614-618
- Lundstrom, I., Shivaraman, S., Svensson, C. & Lundkvist, L. (1975). A hydrogen-sensitive MOS field effect transistor. *Appl. Phys. Lett.*, Vol.26, pp. 55-57
- Lundstrom, K.I. (1981). Hydrogen sensitive MOS-Structures: Principles and Applications. *Sensors and Actuators*, Vol. 1, pp. 403-426
- Lundstrom, I., Armgarth, M. & Petersson, L.-G. (1989). Physics with catalytic metal gate chemical sensors. *CRC Crit. Rev. Sol. State Mater. Sci.*, Vol. 15, No. 2, pp. 201-278
- Silbey, J., Alberty, R.A. (2001). *Physical Chemistry*. New York, Wiley
- Smith, D., Falconer, R., Wittman, E. L. & Vetelino, J. F. (1993). Stability, sensitivity and selectivity of tungsten trioxide films for sensing applications. *Sensors and Actuators B*, Vol. 13-14, pp. 264-268
- Spetz, L., Baranzahi, A., Tobias, P. & Lundstrom, I. (1997). High Temperature Sensors Based on Metal-Insulator-Silicon Carbide Devices. *Physica Status Solidi (a)*, Vol. 162, p. 493
- Spetz, A.L., Tobias, P., Baranzahi, A., Martensson, P. & Lundstrom, I. (1999). Current status of silicon carbide based high-temperature gas sensors. *IEEE Trans. Electron Devices*, Vol.46, No. 3, pp. 561-566
- Spetz, A. L., Tobias, P., Uneus, L., Svenningstorp, H., Ekedahl, L.-G. (2000). High temperature catalytic metal field effect transistors for industrial application. *Sensors and Actuators B*, Vol. 70, pp. 67-76
- Steele, M. C., Hile, J. W. & MacIver, B. A. (1976). Hydrogen-sensitive palladium gate MOS capacitors. *J. Appl. Phys.*, Vol. 47, pp. 2537-2538
- Steele, M. C. & MacIver, B. A. (1976). Palladium/cadmium-sulfide Schottky diodes for hydrogen detection. *Appl. Phys. Lett.*, Vol. 28, pp. 687-688

- Tang, W. M., Lai, P. T., Xu, J. P., Chan, C. L. (2005). Enhanced hydrogen-sensing characteristics of MISiC Schottky-diode hydrogen sensor by trichloroethylene oxidation. *Sensors and Actuators A*, Vol. 119, pp. 63-67
- Tang, W.M., Leung, C.H., Lai, P.T. (2008). Improved sensing characteristics of MISiC Schottky-diode hydrogen sensor by using HfO<sub>2</sub> as gate insulator. *Microelectronics Reliability*, Vol. 48, pp. 1780-1785
- Tobias, P., Baranzahi, A., Spetz, A.L. (1997). Fast chemical sensing with metal-insulator silicon carbide structures. *IEEE Electron Device Lett.*, Vol.18, No. 6, pp. 287-289
- Tomchenko, A. A., Harmer, G. P., Marquis, B. T. & Allen, J. W. (2003). Semiconducting metal oxide sensor array for the selective detection of combustion gases. *Sensors and Actuators B*, Vol. 93, pp. 126-134
- Xu, J.P., Lai, P.T., Zhong, D.G., Chan, C.L. (2003). Improved hydrogen-sensitive properties of MISiC Schottky Sensor with thin NO-Grown oxynitride as gate insulator. *IEEE Trans. Electron Devices*, Vol. 24, No. 1, pp. 13-15
- Zangoie, S., Arwin, H., Lundstrom, I. (2000). Ozone treatment of SiC for improved performance of gas sensitive Schottky diodes. *Materials Science Forum*, Vol. 338-342, pp. 1085-1088
- Zemel, J.N., Keramati, B., Spivak, C.W. & D'Amico. A. (1981). Non-FET Chemical Sensors. *Sensors and Actuators*, Vol. 1, pp. 427-473

IntechOpen



## **Stoichiometry and Materials Science - When Numbers Matter**

Edited by Dr. Alessio Innocenti

ISBN 978-953-51-0512-1

Hard cover, 436 pages

**Publisher** InTech

**Published online** 11, April, 2012

**Published in print edition** April, 2012

The aim of this book is to provide an overview on the importance of stoichiometry in the materials science field. It presents a collection of selected research articles and reviews providing up-to-date information related to stoichiometry at various levels. Being materials science an interdisciplinary area, the book has been divided in multiple sections, each for a specific field of applications. The first two sections introduce the role of stoichiometry in nanotechnology and defect chemistry, providing examples of state-of-the-art technologies. Section three and four are focused on intermetallic compounds and metal oxides. Section five describes the importance of stoichiometry in electrochemical applications. In section six new strategies for solid phase synthesis are reported, while a cross sectional approach to the influence of stoichiometry in energy production is the topic of the last section. Though specifically addressed to readers with a background in physical science, I believe this book will be of interest to researchers working in materials science, engineering and technology.

### **How to reference**

In order to correctly reference this scholarly work, feel free to copy and paste the following:

W.M. Tang, C.H. Leung and P.T. Lai (2012). A Study on Hydrogen Reaction Kinetics of Pt/HfO<sub>2</sub>/SiC Schottky-Diode Hydrogen Sensors, Stoichiometry and Materials Science - When Numbers Matter, Dr. Alessio Innocenti (Ed.), ISBN: 978-953-51-0512-1, InTech, Available from: <http://www.intechopen.com/books/stoichiometry-and-materials-science-when-numbers-matter/a-study-on-hydrogen-reaction-kinetics-of-pt-hfo2-sic-schottky-diode-hydrogen-sensors->

**INTECH**  
open science | open minds

### **InTech Europe**

University Campus STeP Ri  
Slavka Krautzeka 83/A  
51000 Rijeka, Croatia  
Phone: +385 (51) 770 447  
Fax: +385 (51) 686 166  
[www.intechopen.com](http://www.intechopen.com)

### **InTech China**

Unit 405, Office Block, Hotel Equatorial Shanghai  
No.65, Yan An Road (West), Shanghai, 200040, China  
中国上海市延安西路65号上海国际贵都大饭店办公楼405单元  
Phone: +86-21-62489820  
Fax: +86-21-62489821

© 2012 The Author(s). Licensee IntechOpen. This is an open access article distributed under the terms of the [Creative Commons Attribution 3.0 License](#), which permits unrestricted use, distribution, and reproduction in any medium, provided the original work is properly cited.

IntechOpen

IntechOpen